KERNFORSCHUNGSZENTRUM

KARLSRUHE

Februar 1970 KFK 1197

Institut für Angewandte Kernphysik

Nuclear Spectroscopy Using Radiative Neutron Capture and Neutron-Induced Fission

W. Michaelis

GESELLSCHAFT FÜR KERNFORSCHUNG M. B. H.

KARLSRUHE

KERNFORSCHUNGSZENTRUM KARLSRUHE

Februar 1970 KFK 1197

Institut für Angewandte Kernphysik

Nuclear Spectroscopy Using Radiative Neutron Capture and Neutron-Induced Fission*

von

W. Michaelis

* A lecture prepared for the IAEA Study Group Meeting on Research Reactor Utilization, La Casaccia/Rome, 2 - 6 February 1970.

Gesellschaft für Kernforschung m.b.H., Karlsruhe

Abstract:

It is the purpose of this presentation to sketch with the aid of some typical examples the capabilities and achievements of experiments at research reactors in the field of nuclear spectroscopy. Essentially, this research is performed using the radiative neutron capture reaction or neutron-induced fission. The current techniques and approaches are described very briefly. The following scientific topics have been selected: studies of configuration mixing and two-quasiparticle states in nuclei with deformed equilibrium shape, investigations of shell model configurations in even spherical nuclei and search for new regions of stable deformation or shape-isomers. Future trends are discussed and some recommendations for future activities are given.

Der vorliegende Vortrag soll an Hand einiger typischer Beispiele eine kurze Darstellung der Leistungsfähigkeit und Erfolge kernspektroskopischer Experimente an Forschungsreaktoren geben. Solche Forschungsarbeiten machen im wesentlichen Gebrauch von der Neutroneneinfangreaktion oder der Neutronen-induzierten Kernspaltung. Der Stand der Technik und der Methoden wird kurz beschrieben. Folgende wissenschaftliche Fragestellungen wurden für die Diskussion ausgewählt: Untersuchungen von Konfigurationsmischungen und Zwei-Quasiteilchen-Zuständen in deformierten Kernen, Untersuchungen von Schalenmodell-Konfigurationen in geraden sphärischen Kernen sowie die Suche nach neuen Massenbereichen mit stabiler Deformation oder Gestaltisomeren. Der Beitrag schließt mit einer Diskussion zukünftiger Trends und einigen Anregungen für weitere Aktivitäten auf diesem Gebiet.

1. Introduction

During the past few years there has been a considerable progress in nuclear physics experiments at research reactors. Nuclear spectroscopy studies using radiative neutron capture or neutron-induced fission now yield a degree of insight into the nucleus which could not have been imagined some years ago. To a great extent, this progress has become possible by the rapid development of semiconductor detector technology and associated electronics. The realization of lithium-drifted germanium detectors has enabled high-resolution gamma-ray spectroscopy with fairly good efficiency up to 10 MeV photon energy. The availability of detectors with sensitive volumes up to 70 cm^3 allows to perform high-resolution multiparameter experiments with these devices. Silicon detectors have made possible the spectroscopy of heavy ions and thus the study of radiation emitted from fission fragments of specific mass. Other important advances are the considerable improvements achieved in coherent scattering process instruments, in magnetic internal conversion electron spectrometers, in magnetic mass separators for fission products and in fast radiochemical separation techniques.

It is the purpose of this presentation to describe with the aid of some examples the scientific achievements of present techniques and to illustrate the purpose behind this research.

2. Current Techniques and Approaches

A detailed survey on present techniques and approaches is given in other lectures of this meeting. Therefore the discussion may be here very brief and may be restricted to methods which have been used in the research described in the following sections.

The potential of lithium-drifted germanium counters has been considerably increased by operating the detectors in Compton-suppression mode [1]⁺. In this technique the germanium counter is surrounded by a scintillation detector and Compton events are eliminated to a large extent by means of an anticoincidence circuit. The range of application is usually between 100 keV and 3 MeV and accuracies of 50 eV or better in the gamma-ray energy determination are now obtainable using computer analysis of the measured spectra. In neutron-capture spectroscopy anti-Compton spectrometers thus provide very powerful complementary instruments to coherent scattering spectrometers [2] which possess uncontested characteristics below about 500 keV [1,2,3]. Fig.1 shows a typical sectional display of a gamma-ray spectrum obtained with an anti-Compton spectrometer [3]. The example clearly demonstrates both the high resolution and the effective suppression of Compton events. This technique allows the application of the Ritz combination principle to excitation energies of several MeV.

Another important piece of information for establishing the capture gamma-ray transition diagram is provided by high-resolution measurements in the upper part of the capture spectrum. The identification of levels is quite direct when one assumes that the transitions which are in energy close to the neutron separation energy proceed from the neutron-capture state. Line widths (FWHM) of 4.5 keV at 5.5 MeV and 5.1 keV at 6.9 MeV have been achieved [4]. An example is shown in Fig.2 .

In another class of experiments the random fluctuations in intensity for the primary gamma rays are averaged out by measuring the spectra that result from the capture of neutrons in an energy band containing many resonances [5,6]. Such measurements reveal the parity of low-lying nuclear states and also restrict the spin assignment in general to two possible values.

⁺ The literature given in this section is certainly not exhaustive. It is restricted to papers of recent date. As to the earlier works we refer to the literature cited in the given refs.

Gamma-gamma coincidence measurements in neutron capture spectroscopy have been developed to a high degree of efficiency using either the combination Ge(Li)-NaI(Tl) or Ge(Li)-Ge(Li) [7,8,9]. The use of on-line computers is of considerable aid in these experiments, since the possibility of setting digital windows in a very versatile manner permits the systematic application of the window subtraction method [8,9,10]. A typical example for a quite unfavourable case is illustrated in Fig.3 . The gamma rays at 876 keV and 1173 keV in ^{62}Ni occur in coincidence. Accordingly, the 1173 keV line is well pronounced in the lower spectrum of Fig.3, while the 876 keV peak clearly disappears [11].

Information on level spins and multipole mixing parameters may be obtained by measuring the angular correlation of gamma-ray cascades [12]. Here also the use of on-line computers and the application of the window subtraction method are of great advantage. A large number of cascades can be measured simultaneously [13]. This provides an extensive set of data which allows the mutually consistent determination of many level spins and multipole mixtures. The angular correlations can be displayed on a CRT during the measurement so that a full evaluation of the state of the experiment is possible at any time (Fig.4).

Quite direct insight into the nuclear wave functions may be obtained by determining the partial gamma-ray halflives [14,15]. Due to their superior timing capabilities fast scintillators have been preferably used in halflife measurements [16,17].

As to other important techniquessuch as internal conversion electron measurements, experiments with polarized neutrons and the use of nuclear orientation which have not been discussed here we refer to the recent articles [18,19,20] and the literature cited there.

In fission physics the development of magnetic mass separators has made possible the mass separation of fission products and thus nuclear spectroscopy on neutron-rich nuclei far off the stability line

[21]. Since the flight time through the separator is in the order of 1 μ sec, the instruments allow the study of isomeric gamma emission with halflives $>$ 1 μ sec and the investigation of the fission product beta decay. Rapid radiochemical separation techniques have successfully attacked separation times in the order of 1 sec [22,23]. For studying the prompt deexcitation of individual primary fission fragments it is necessary to perform three-parameter experiments in which, e.g., a large-volume Ge(Li) detector is used for high-resolution gamma-ray spectroscopy and the coincident fission-fragment masses are deduced from the correlated kinetic energies as measured by two Si solid-state detectors [24]. The observable Doppler shift in gamma-ray energy allows the assignment of lines to single members of fragment pairs. A schematic view of an experimental set-up is shown in Fig. 5 .

3. Nuclear Spectroscopy on Deformed Nuclei Using Radiative Neutron Capture

Let us select in this field two nuclear structure problems which are attracting increasing attention: the problem of state mixing and that of two-quasiparticle excitations.

With increasing quantity and detail of experimental data on nuclear excitations the simple picture that assumes pure nuclear states with neglect of configuration mixing leads to serious disagreement between theoretical predictions and empirical results. A better understanding of the various phenomena requires systematic experimental and theoretical studies. On the experimental side, neutron capture gamma-ray spectroscopy can provide valuable contributions to this problem. Although level information may be obtained in a more direct manner from other nuclear reactions, the neutron capture process permits a more detailed study of the level decay without restriction to any particular mode of excitation. We shall present several examples in the following paragraphs. Theoretically, various attempts have been made in the past to extend the simple picture of pure nuclear states. A model which has proved to be very successful in interpreting the experimental results on deformed odd-mass nuclei has been described in refs. [14,15,25]. The model includes quasiparticle-phonon interaction, Coriolis coupling, rotation-vibration interaction and pairing correlations. It predicts the energy and structure of individual levels, branching ratios for gamma-ray transitions, multipole mixtures and partial gamma-ray halflives. We shall use this model when comparing the experimental results with theoretical predictions.

Fig.6 shows the transition diagram of ^{167}Er as reported in refs. [15,26]. The diagram which considerably extends our knowledge of the nucleus ^{167}Er is based on precision measurements in the lower and upper part of the capture spectrum and on gamma-gamma coincidence studies. An enriched sample of ^{166}Er was used as a target (σ = 45 ± 9 b). A large number of levels have been identified and have been assigned to specific configurations and their superimposed rotational bands. Detailed analysis of the data suggests strong mixing between Nilsson states and the quadrupole vibrations Q_{22}, Q_{2-2} and Q_{20}. As an example let us select the deexcitation of the $1/2^-$ rotational band observed at 763 keV. The only Nilsson state with spin and parity $1/2^-$ near the Fermi level is the orbit $1/2^-[521]$. This state, however, is well established to occur at 208 keV excitation energy. Thus it is reasonable to assume that the band at 763 keV corresponds to the Q_{2-2} gamma-vibrational band based upon the configuration $5/2^-[512]$ and, in fact, a collective E2 transition leaving the bandhead is observed. In other respects, however, the deexcitation shows clear anomalies. From both the first and second member of the band transitions proceed to the $1/2^-[521]$ Nilsson band which in intensity considerably exceed the E2 transitions to the "own" intrinsic configuration. In addition, the branching ratio to the $3/2^-$ and $1/2^-$ levels is exceptional. A reasonable explanation for these anomalies is provided by assuming a strong admixture of the $1/2^-[510]$ Nilsson state in the $5/2^-[512]$ + Q_{2-2} excitation. Though the $1/2^-[510]$ orbit is expected at much higher energies, this admixture can be understood within a microscopic picture of the quadrupole vibrations. In this picture the collective excitation has to be considered as a superposition of one-quasiparticle states, three-quasiparticle states and more complex configurations. Since the $1/2^-$[510] orbit is connected with the $5/2^-$[512] state by a large E2 matrix element, one has to expect a strong admixture of the $1/2^-$[510] state in the quadrupole vibration. Calculations predict an admixture of 38 % and the branching ratios calculated with inclusion of configuration mixing are in quite good agreement with the experimental observation [15,26]. Similar considerations can be made on other rotational bands.

Information on band mixing may also be obtained from the partial gamma-ray halflives which in many cases (in particular K-forbidden transitions) are very sensitive to small admixtures in the wave functions [14,15]. This is demonstrated in Table 1 where the theoretical values are compared with experimental data. H' = 0 refers to the adiabatic model, whereas H' $\neq$ 0 denotes the model described above. It is shown in the Table that the experimental values which have been quoted from refs. [16,17] reveal fairly good agreement with theory, when configuration mixing is fully taken into account.

With regard to the investigation of two-quasiparticle excitations let us select the nucleus ^{168}Er. The low-energy spectrum of the reaction ^{167}Er(n,γ)^{168}Er has been studied extensively by means of a bent-crystal diffraction instrument [27]. Using a Ge(Li) anti-Compton spectrometer the detail and quality of the data has been considerably improved in the energy range 500 to 2000 keV [3]. Additional information has come from measurements of the high-energy spectrum with thermal neutrons [3] and with neutrons in an energy band containing many resonances [5]. On the basis of these investigations a very detailed transition diagram up to 2 MeV has been established which allows definite conclusions on the spectroscopic interpretation of many excited states. The diagram as reported in ref. [3] is shown in Fig.7 . Of particular interest is the energy range from 1 to 2 MeV, since for most

Table 1

Partial gamma-ray halflives [14,15]

Nucleus	Initial configuration	Final configuration	$T_{1/2\gamma}$ (nsec)		
			H'=0	H'≠0	Exp.
^{169}Yb	$\frac{5}{2}^- \frac{5}{2}$ [512]	$\frac{1}{2}^- \frac{1}{2}$ [521]	$2.1 \cdot 10^4$	630	102[a] 320[b]
		$\frac{3}{2}^- \frac{1}{2}$ [521]	$1.9 \cdot 10^5$	135	103[a] 260[b]
		$\frac{5}{2}^- \frac{1}{2}$ [521]	$6.3 \cdot 10^5$	110	84[a] 220[b]
^{167}Er	$\frac{5}{2}^- \frac{5}{2}$ [512]	$\frac{1}{2}^- \frac{1}{2}$ [521]	$8.3 \cdot 10^4$	517	c
		$\frac{3}{2}^- \frac{1}{2}$ [521]	$1.0 \cdot 10^6$	85	c
		$\frac{5}{2}^- \frac{1}{2}$ [521]	$5.7 \cdot 10^6$	99	c

[a] Ref. [17] [b] Ref. [16]

[c] Experimental values not yet available.

of the nuclei in this mass region the knowledge of the high-lying configurations is still very poor. It is beyond the scope of this presentation to give a detailed discussion here. Let us therefore select some interesting points.

The rotational bands at 1354 keV, 1569 keV and 1542 keV have to be identified with the $K^\pi = 1^-$, 2^- and 3^- octupole vibrational bands and the 3^- rotational member of the $K^\pi = 0^-$ octupole band most probably occurs at 1914 keV. The properties of the $K^\pi = 1^-$ and $K^\pi = 3^-$ states are presumably close to those of two-quasiparticle states. These states are the neutron levels $[512\uparrow - 633\downarrow]_{nn}$ and $[633\uparrow - 521\downarrow]_{nn}$. The energies within the $K^\pi = 1^-$ band do not follow the simple rotational-energy systematics. This is due to strong Coriolis coupling within the octupole bands, in particular with the $K^{\pi} = 0^-$ state. We can compare the structure and excitation energies with the predictions of various microscopic models (pairing plus state-independent octupole force, surface delta interaction, pairing plus octupole force). The measurements therefore reveal significant data for the microscopic theory of the nucleus.

Another important experimental result is the verification of a $K^{\pi} = 0^+$ band at 1217 keV. Within the model of pairing plus quadrupole and spin-quadrupole force one obtains from this band the interaction constants $\mathcal{K}_q = 5.3$ and $\mathcal{H}_t = 8.8$ (in units of $A^{-1/3}\hbar\omega_0$). From the gamma-vibrational band we get $\mathcal{H}_q = 4.6$ and $\mathcal{H}_t = 5.4$. These values then may be used to predict other collective two-quasiparticle configurations and the results may be compared with the experimental decay scheme [3]. Again we see that the measurements yield important data for a better understanding of the nuclear many-particle problem. Till now there are only very few nuclei where the excitation spectrum above 1 MeV is sufficiently known. Since the levels in this energy region are well populated in neutron capture, this reaction provides a powerful tool for studying such excitations.

4. Nuclear Spectroscopy on Spherical Nuclei Using Radiative Neutron Capture

Fig.8 shows the transition diagram of ^{62}Ni as reported in ref. [11]. The diagram is based essentially on coincidence relationships and the level spins have been determined by γ-γ angular correlation measurements. A highly enriched sample of ^{61}Ni was used in this investigation. The capture cross section of ^{61}Ni is only 2.0 b. Nevertheless a large number of levels have been identified with energies up to 5 MeV. The purpose of such investigations is to check the predictions of more or less realistic nuclear models in this mass region.

^{62}Ni is in the vicinity of doubly closed shells and is considered to be spherical. In earlier macroscopic descriptions the low-lying excited states have been interpreted as surface oscillations and, indeed, some regularities in the spectra of the even nuclei in this region together with strongly enhanced E2 transition strengths seem to support the collective picture. However, several investigations have shown that the success of this picture is very limited and several attempts have been made to understand the structure of these nuclei from the microscopic point of view. Of particular importance within such more realistic models are various exact shell model calculations /28,29,30,31/. Fig.9 gives a comparison of theoretical predictions with the experimental level scheme of ^{62}Ni. The common basis of the calculations is to assume a closed core of ^{56}Ni, to restrict the additional neutrons to the 2 p 3/2, 1 f 5/2 and 2 p 1/2 orbits and to hope to absorb the interactions with the core into effective residual interactions between the valence neutrons. The calculations differ in the choice of the nucleon-nucleon potential and in the parametrization. We see that in spite of the common basis the predictions differ remarkably and that a detailed knowledge of the experimental level scheme is essential for checking the theoretical treatment.

Much more sensitive to the interactions used in the calculations are the reduced transition probabilities rather than the level positions. Of particular interest is the ratio

$$b = \frac{B\ (E2;\ 2_2^+ \rightarrow 2_1^+)}{B\ (E2;\ 2_2^+ \rightarrow 0_1^+)} .$$

In earlier decay investigations only an upper limit could be given for this value, since the E2 content in the $2_2^+ \rightarrow 2_1^+$ transition was unknown. The angular correlation measurements in ref. /11/ revealed $11 < b < 23$. The theoretical values predicted in refs. /30/ and /31/

are b = 33 and b = 1310, respectively. The large difference clearly demonstrates the sensitivity to the interactions used. The agreement of the first value with the experimental result has to be considered as quite satisfactory. The large number of branching ratios and multipole mixtures which can be determined in neutron capture [8,11,13] allow to extend these considerations to other transitions, but there is still a lack of theoretical predictions.

5. Nuclear Spectroscopy Using Neutron-Induced Fission

If we compare the conventional chart of the nuclides with the lines of vanishing proton and neutron separation energies, we learn that the number of nuclei which have not been investigated so far considerably exceeds the number of nuclei which have already been studied with some success. Therefore, it is attractive to extend the methods of nuclear spectroscopy to regions far off the stability line. Such investigations will certainly increase the understanding of the many-particle problem "nucleus". A powerful means for producing neutron-rich nuclei which are not accessible by usual nuclear reactions is provided by the fission process. Let us select here one very interesting and topical problem: the search for new regions of deformation.

There are both theoretical and experimental hints that around mass number 110 a new region of deformation occurs. Already several years ago a regular structure in delayed gamma-ray spectra measured with poor resolution was observed by applying appropriate mass selection to the fission fragments in spontaneous fission of ^{252}Cf [32]. This structure is in good agreement with the assumption of rotational cascades. Very recently in ref. [33] gamma-ray transitions in six adjacent Ru isotopes have been examined with Ge(Li) detectors using a recoil chemical method in neutron-induced fission of ^{235}U. In ^{106}Ru, ^{107}Ru and ^{108}Ru purely rotational level schemes can consistently account for the observed transition energies, halflives and coincidence relation-

Table 2

Tentative interpretation of the gamma rays as rotational transitions [37]

Most probable nucleus	Eγ (keV) exp.	Eγ (keV) calc.	Intensity[a] Iγ	$J_i \rightarrow J_f$	$\frac{\hbar}{2\Theta}$ (keV)
$^{104}_{42}Mo$	191 ± 2	191	12 ± 4	4 → 2	13.6
	296 ± 2[b]	300	8.8 ± 2.9	6 → 4	
	c	409		8 → 6	
	518 ± 3	518	15 ± 7.5	10 → 8	
$^{102}_{42}Mo$ or $^{102}_{40}Zr$	174 ± 2	176	7.7 ± 2.6	4 → 2	12.6
	275 ± 2	277	7.6 ± 2.6	6 → 4	
	c	378		8 → 6	
	c	479		10 → 8	
	581 ± 4	580	15 ± 7.5	12 → 10	
$^{103}_{41}Nb$	136 ± 2	135	7.8 ± 2.7	$\frac{11}{2} \rightarrow \frac{9}{2}$	12.3
	157 ± 2	160	5.4 ± 1.8	$\frac{13}{2} \rightarrow \frac{11}{2}$	

[a] Relative intensity per fission and ≈ 16 mm flight path.

[b] Alternative interpretation: crossover transition in $^{103}_{41}Nb$. Possibly doublet.

[c] Possibly obscured by complex structures.

ships. However, attempts to excite the rotational levels in ^{106}Ru by means of (t,p) and Coulomb excitation techniques revealed no indications for a rotational structure [34]. Therefore, one might speculate on the possibility of the existence of so-called shape-isomers. In this connection it would be interesting to look at isomeric gamma emission in this mass region and, indeed, isomeric gamma rays have been observed with a gas-filled mass separator for mass numbers between 98 and 102 [35]. However, the correspondence in the masses is unsatisfactory and the problem remains still unsettled. In ref. [24] the technique of high-resolution three-parameter experiments which was first used in spontaneous fission [36] has been extended to neutron-induced fission. Very recently detailed analysis of the data for the mass range 102 to 104 (cf. Fig.10) revealed evidence for rotational systematics in the associated gamma-ray spectra [37]. A tentative interpretation of the observed transitions is given in Table 2. The systematic behaviour of the energy values and the similarity of the deduced rotational factors are conspicuous. However, there are also serious objections against this interpretation. In particular, the absolute values of the rotational factors seem to be rather low for this mass region and the quite good following of the simple J(J+1) rule is surprising in view of the fact that e.g. ^{100}Mo is still nearly spherical (E_{2^+} = 536 keV). In any case the question whether we are dealing with a deformed ground-state or excited state is still unsolved and further experimental data are required.

In summary, we can conclude from this brief discussion that quite exciting problems can be tackled in nuclear spectroscopy using the fission process.

6. Trends and Recommendations

All the experiments sketched in the preceding sections have been performed using research reactors with maximum thermal fluxes between 10^{13} and 10^{14} n/cm^2 sec. Future experiments have to start from the fact that very soon several reactors with much higher fluxes will be available. Such reactors offer great advantages in particular in high-precision measurements of neutron-capture singles spectra and in multiple-parameter fission experiments. When using smaller reactors, it is therefore quite essential to put much effort in the intensity optimization. Singles spectra measurements should apply internal target geometry and, where external targets are needed, the filtered beam method or the use of neutron guide tubes is recommended. Pure neutron beams between 10^8 and 10^9 n/cm^2 sec can be obtained with the above thermal fluxes [38].

It is evident from the foregoing discussions that in general reliable conclusions with respect to interesting nuclear problems can be achieved only by applying several techniques which are complementary to each other. Therefore it is convenient either to install several instruments at the same reactor or to coordinate the research work with other laboratories.

It is believed that on the basis of the presently known techniques neutron capture gamma-ray spectroscopy will continue to be an important field of research during the next five or six years. There will be an increasing tendency to study nuclei with smaller cross sections, to use highly enriched isotopes and to extend the investigations to higher excitation energies. Large volume Ge(Li) detectors will therefore play a very important role. The use of small or medium-size computers in two- or multiple-parameter experiments is highly recommended. This technique not only involves great advantages for the measurements, but also offers the possibility for a basic training of graduate students and young scientists in the important field of computer application and associated problems.

Nuclear spectroscopy using neutron-induced fission is still a young field of activity and will certainly attract much effort for a long period of time. Further investigations and improvements of the methods in fast chemistry and other separation techniques are desirable and a lot of data has still to be accumulated. While most of this research can be pushed forward with moderate neutron fluxes, multiple-parameter experiments will probably provide promising results only if the flux is 10^{14} n/cm^2 sec or better. A wide field of studies is possible in this kind of experiment. In addition to gamma rays conversion electrons and X-rays should be studied. Different geometries may be used and the radiation emitted should be examined in different time intervals after fission.

References:

/1/ W. Michaelis and F. Horsch, "Neutron Capture Gamma-Ray Spectroscopy", IAEA Vienna, 1969, p.35

/2/ H.R. Koch, H. Baader, D. Breitig, U. Gruber, B.P.K. Maier and O.W.B. Schult, Contributions Int.Conf. on Properties of Nuclear States, Montreal 1969, p.144

/3/ W. Michaelis, H. Ottmar and F. Weller, Nucl.Phys. (in press)

/4/ H. Ottmar, to be published

/5/ L.M. Bollinger and G.E. Thomas, Phys.Rev.Lett. 21 (1968) 233; "Neutron Capture Gamma-Ray Spectroscopy", IAEA Vienna, 1969

/6/ R.C. Greenwood, "Neutron Capture Gamma-Ray Spectroscopy", IAEA Vienna, 1969

/7/ H.H. Bolotin, "Neutron Capture Gamma-Ray Spectroscopy", IAEA Vienna, 1969

/8/ U. Fanger, W. Michaelis, H. Schmidt and H. Ottmar, Nucl.Phys. A128 (1969) 641

/9/ D. Heck, to be published

/10/ U. Fanger, KFK 887

/11/ U. Fanger, D. Heck, W. Michaelis, H. Ottmar, H. Schmidt and R. Gaeta, Nucl.Phys. (in press)

/12/ H. Schmidt and D. Heck, "Neutron Capture Gamma-Ray Spectroscopy", IAEA Vienna, 1969, p.371

/13/ H. Schmidt, W. Michaelis and U. Fanger, Nucl.Phys. A136 (1969) 122

/14/ W. Michaelis, F. Weller, H. Schmidt, G. Markus and U. Fanger, Nucl.Phys. A119 (1968) 609

/15/ W. Michaelis, F. Weller, U. Fanger, R. Gaeta, G. Markus, H. Ottmar and H. Schmidt, Nucl.Phys. (in press)

/16/ K.E.G. Löbner and S.G. Malmskog, Nucl.Phys. 80 (1966) 505

/17/ H. Nabielek, SGAE PH-78/1968

/18/ T. von Egidy, "Neutron Capture Gamma-Ray Spectroscopy", IAEA Vienna, 1969

/19/ J. Kopecky, F. Stecher-Rasmussen and K. Abraham, Contributions Int.Conf. on Properties of Nuclear States, Montreal 1969, p.133

/20/ H. Postma, E.R. Reddingius and J. Mellema, Contributions Int. Conf. on Properties of Nuclear States, Montreal 1969, p.109

/21/ P. Armbruster, J. Eidens and E. Roeckl, Arkiv för Fysik 36, No.37 (1966) 293

/22/ G. Herrmann, Arkiv för Fysik 36, No.14 (1966) 111

/23/ G. Zicha, K.E.G. Löbner, P. Maier-Komor, J. Maul and P. Kienle, Contributions Int.Conf. on Properties of Nuclear States, Montreal 1969, p.83

/24/ F. Horsch and W. Michaelis, "Physics and Chemistry of Fission", IAEA Vienna 1969, p.527

/25/ F. Weller, Thesis, University Heidelberg 1970; Nucl.Phys., to be published

/26/ W. Michaelis, F. Weller, H. Ottmar, U. Fanger, R. Gaeta and H. Schmidt, "Neutron Capture Gamma-Ray Spectroscopy", IAEA Vienna 1969, p.469

/27/ H.R. Koch, Z.Physik 192 (1966) 142

/28/ L.S. Hsu and J.B. French, Phys.Lett. 19 (1965) 135; L.S. Hsu, Nucl.Phys. A96 (1967) 624

/29/ A. Plastino, R. Arvieu and S.A. Moszkowski, Phys.Rev. 145 (1966) 837

/30/ S. Cohen, R.D. Lawson, M.H. Macfarlane, S.P. Pandya and M. Soga, Phys.Rev. 160 (1967) 903

/31/ N. Auerbach, Phys.Rev. 163 (1967) 1203

/32/ S.A.E. Johansson, Nucl.Phys. 64 (1965) 147

/33/ G. Zicha, K.E.G. Löbner, P. Maier-Komor, J. Maul and P. Kienle, Contributions Int.Conf. on Properties of Nuclear States, Montreal 1969, p.83; G. Zicha, Thesis, University Munich 1969

[34] P. Kienle, unpublished

[35] P. Armbruster, "Physics and Chemistry of Fission", IAEA Vienna 1969, p. 543

[36] R.L. Watson, UCRL-16798 (1966)

[37] F. Horsch, to be published

[38] F. Horsch and I. Piper, KFK 1003 (1969)

Figure Captions:

Fig.1 Sectional display of the neutron-capture spectrum from a natural erbium sample as measured with an anti-Compton spectrometer [3]. The inset illustrates the computer analysis for a group of gamma rays using modified Gaussian functions.

Fig.2 High-energy capture spectrum from a sample of enriched ^{95}Mo in the energy range from 4.9 to 8.7 MeV showing 4.5 keV FWHM energy resolution at 5.5 MeV [4].

Fig.3 $^{61}Ni(n,\gamma)^{62}Ni$: Two Ge(Li) spectra in coincidence with γ lines observed with a NaI(Tl) detector. The digital window positions in the NaI spectrum are indicated in the inset. The lower and upper spectrum are coincident with lines at 876 keV and 1173 keV, respectively, and have been obtained by means of the window subtraction method [11].

Fig.4 Angular correlation of the (848 + 850) - 778 keV cascade from $^{95}Mo(n,\gamma)^{96}Mo$ displayed on CRT [12].

Fig.5 Schematic view of an experimental set-up for studying the prompt gamma rays emitted from individual fragments in neutron-induced fission [24].

Fig.6 Gamma-ray transition diagram of ^{167}Er [15,26].

Fig.7 Transition diagram of ^{168}Er as reported in ref. [3].

Fig.8 Transition diagram of ^{62}Ni as proposed in ref. [11].

Fig.9 Comparison of the ^{62}Ni level scheme with results of exact shell model calculations.

a) Ref. [31] b) Ref. [30] c) Ref. [28] d) Ref. [29]

Fig.10 Indication for regular structures in the prompt gamma-ray spectra observed for the fragment masses A = 103 ± 1 and A = 131 ± 1. The two spectra represent the cases:

(a) Light fragment moving towards the gamma-ray detector,

(b) heavy fragment travelling towards the gamma-ray detector.

The letters L and H indicate assignments to the light and heavy fragments, respectively.

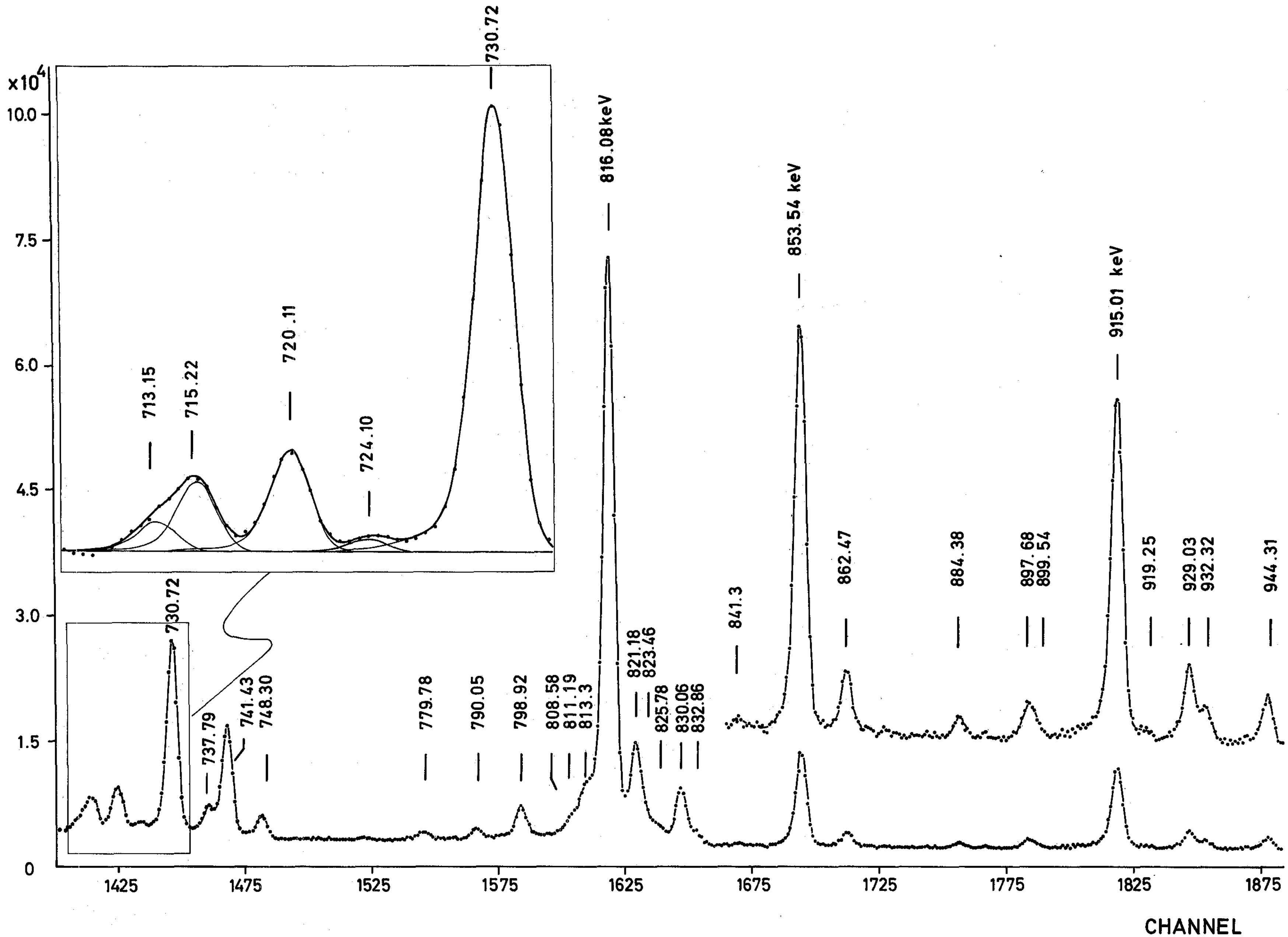
x10^4
10.0
7.5
6.0
4.5
3.0
1.5
0
713.15
715.22
720.11
724.10
730.72
737.79
741.43
748.30
779.78
790.05
798.92
808.58
811.19
813.3
816.08keV
821.18
823.46
825.78
830.06
832.86
841.3
853.54 keV
862.47
884.38
897.68
899.54
915.01 keV
919.25
929.03
932.32
944.31
1425
1475
1525
1575
1625
1675
1725
1775
1825
1875
CHANNEL

Fig.1

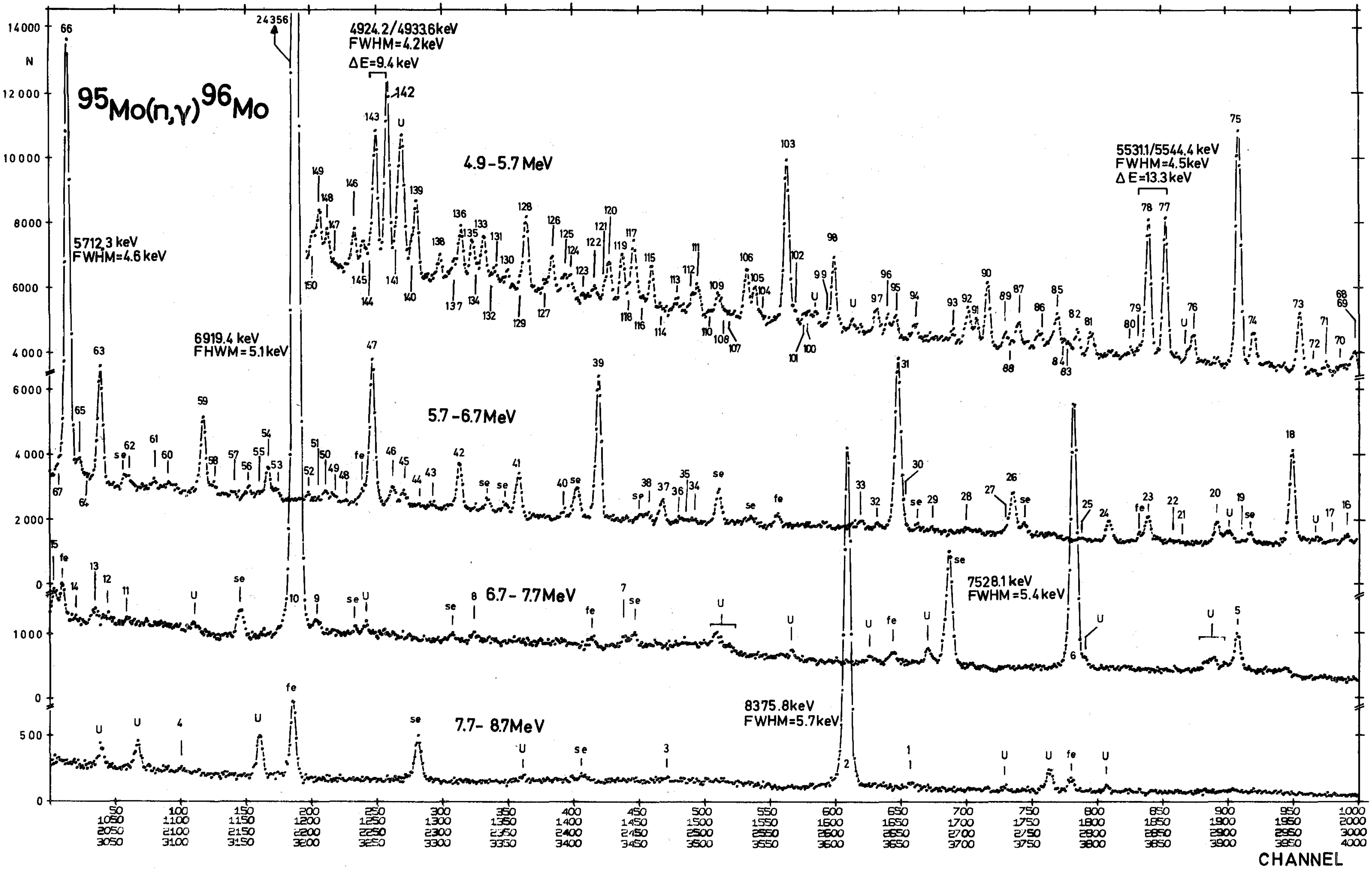

95Mo(n,γ)96Mo
4.9-5.7 MeV
5.7-6.7MeV
6.7- 7.7MeV
7.7- 8.7MeV
4924.2/4933.6keV
FWHM=4.2keV
ΔE=9.4keV
5531.1/5544.4 keV
FWHM=4.5keV
ΔE=13.3keV
5712.3 keV
FWHM=4.6 keV
6919.4 keV
FHWM=5.1keV
7528.1 keV
FWHM=5.4keV
8375.8keV
FWHM=5.7keV
24356
N
CHANNEL

Fig.2

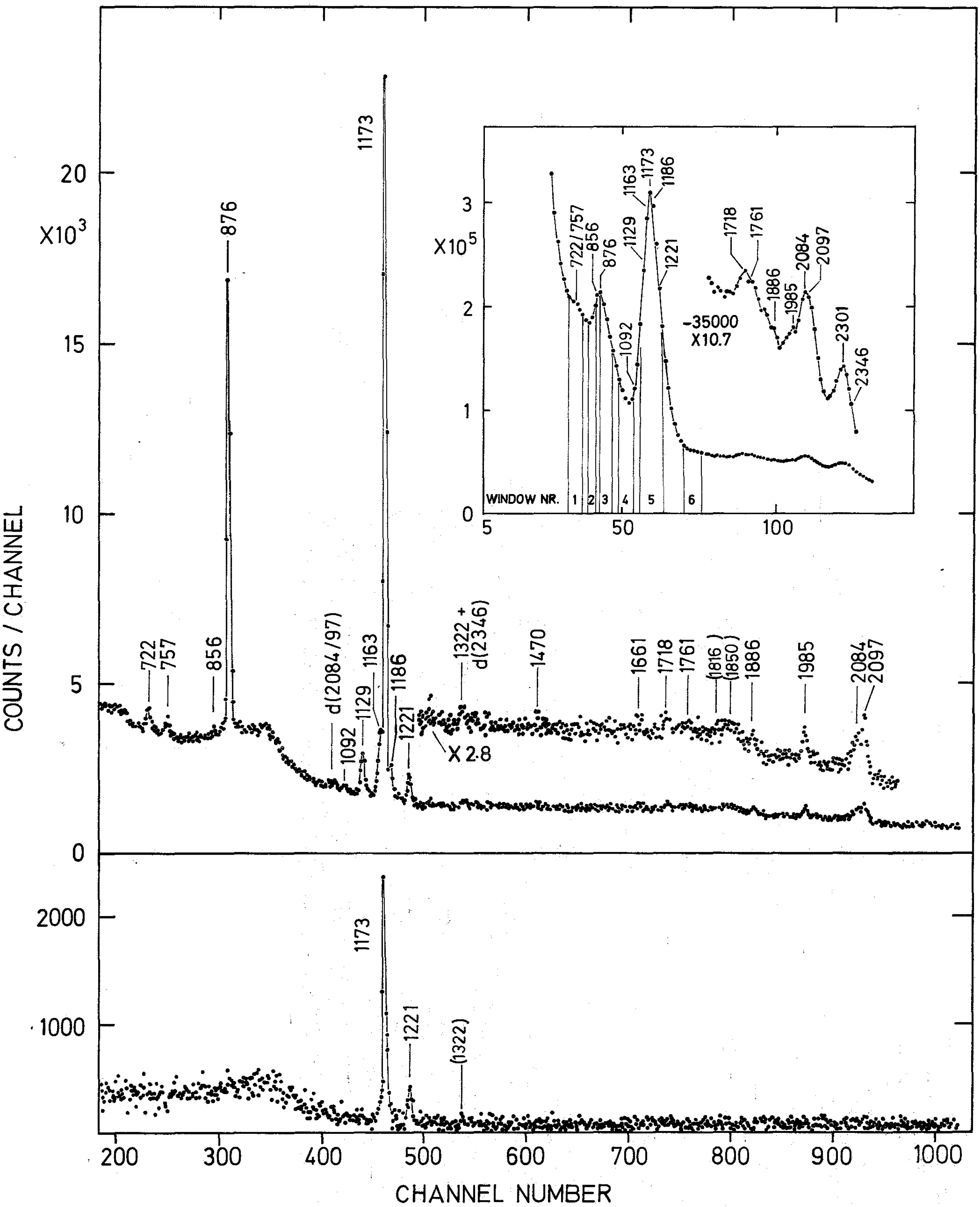
COUNTS / CHANNEL
X10^3
CHANNEL NUMBER
722
757
856
876
d(2084/97)
1092
1129
1163
1173
1186
1221
X 2.8
1322 +
d(2346)
1470
1661
1718
1761
(1816)
(1850)
1886
1985
2084
2097
(1322)
X10^5
WINDOW NR.
722/757
-35000
X10.7
2301
2346

Fig.3

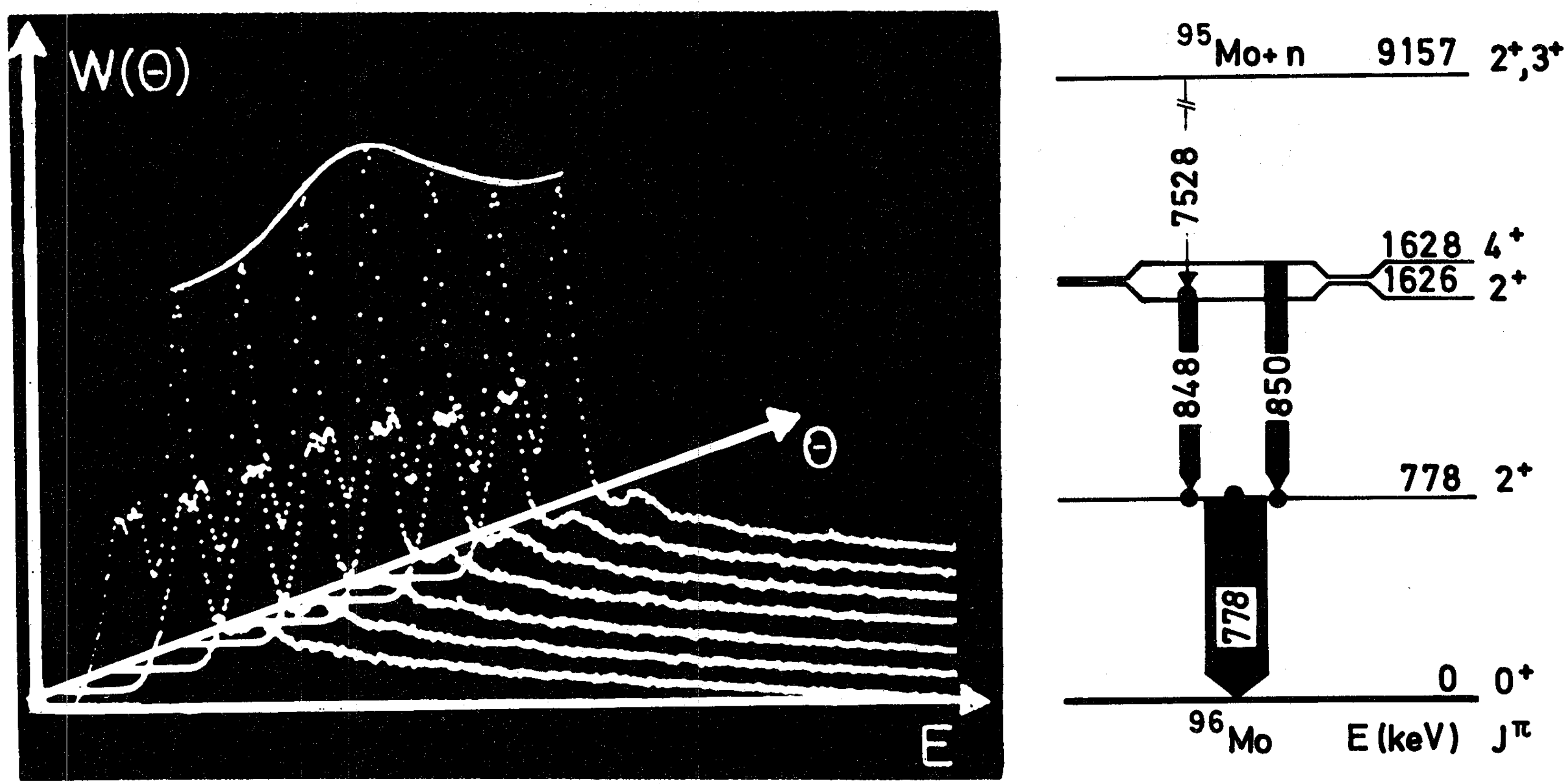

W(Θ)
Θ
E
95Mo+ n
9157
2+,3+
7528
1628
4+
1626
2+
848
850
778
2+
778
0
0+
96Mo
E (keV)
Jπ

Fig. 4

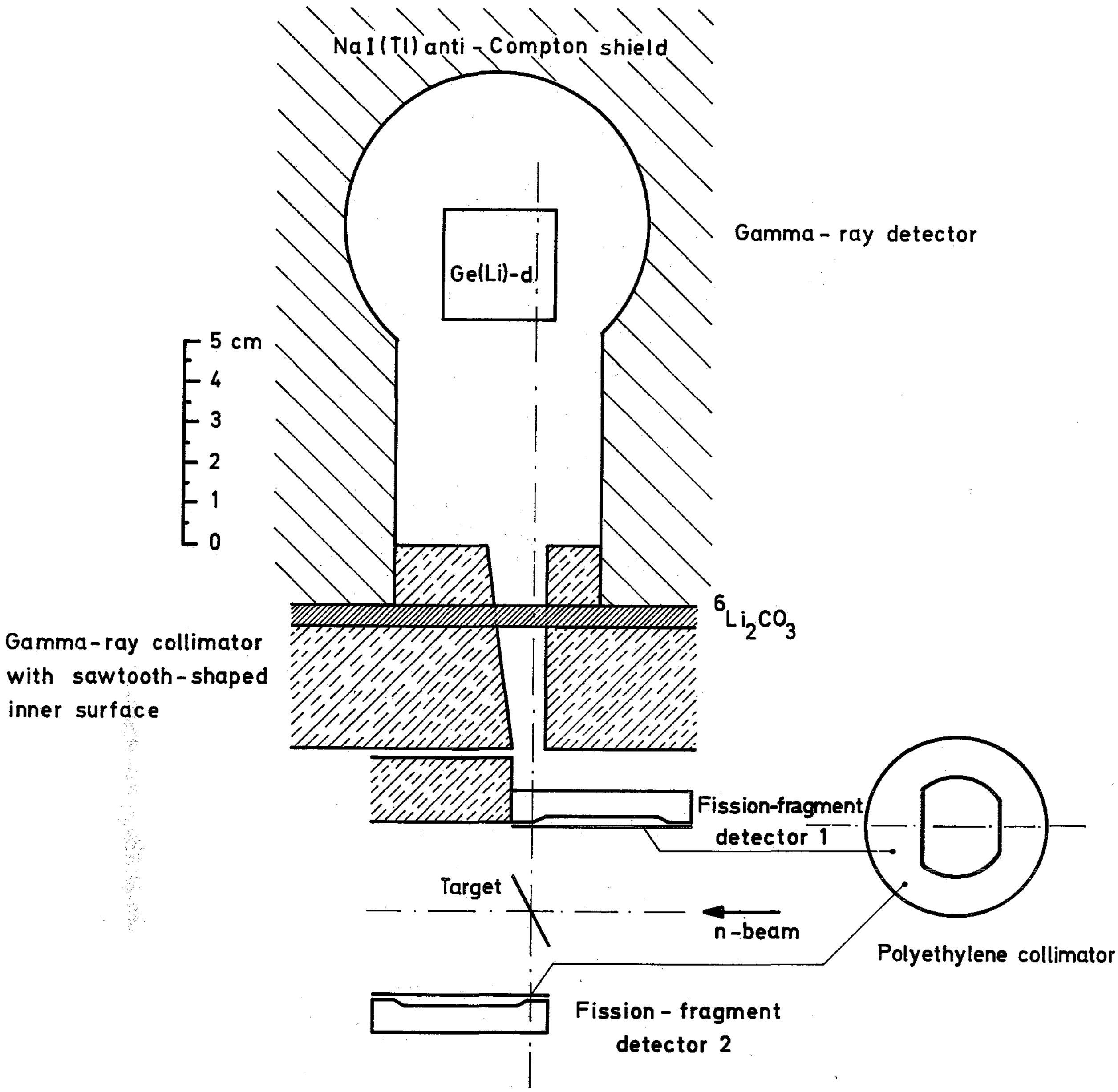

NaI(Tl) anti - Compton shield
Gamma - ray detector
Ge(Li)-d
5 cm
4
3
2
1
0
$^6Li_2CO_3$
Gamma-ray collimator
with sawtooth-shaped
inner surface
Fission-fragment
detector 1
Target
n-beam
Polyethylene collimator
Fission - fragment
detector 2

Fig.5

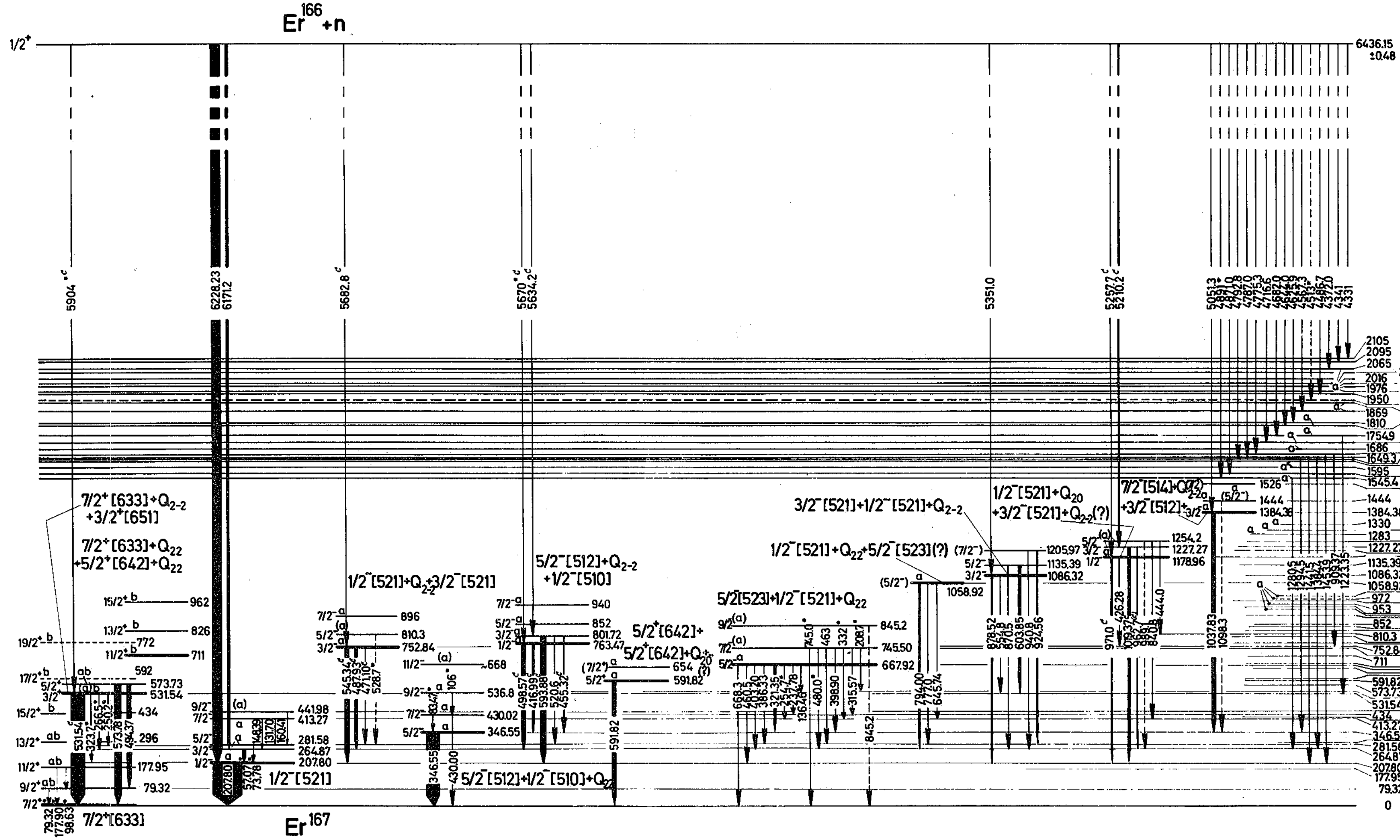
Er166 +n
Er167
1/2+
6436.15 ±0.48
7/2+[633]
1/2−[521]
7/2+[633]+Q2-2 +3/2+[651]
7/2+[633]+Q22 +5/2+[642]+Q22
1/2−[521]+Q22+3/2−[521]
5/2−[512]+Q2-2 +1/2−[510]
5/2−[512]+1/2−[510]+Q22
5/2+[642]+
5/2+[642]+Q20
5/2−[523]+1/2−[521]+Q22
1/2−[521]+Q22+5/2−[523](?)
3/2−[521]+1/2−[521]+Q2-2
1/2−[521]+Q20 +3/2−[521]+Q22(?)
7/2−[514]+Q22 +3/2−[512]+

Fig.6

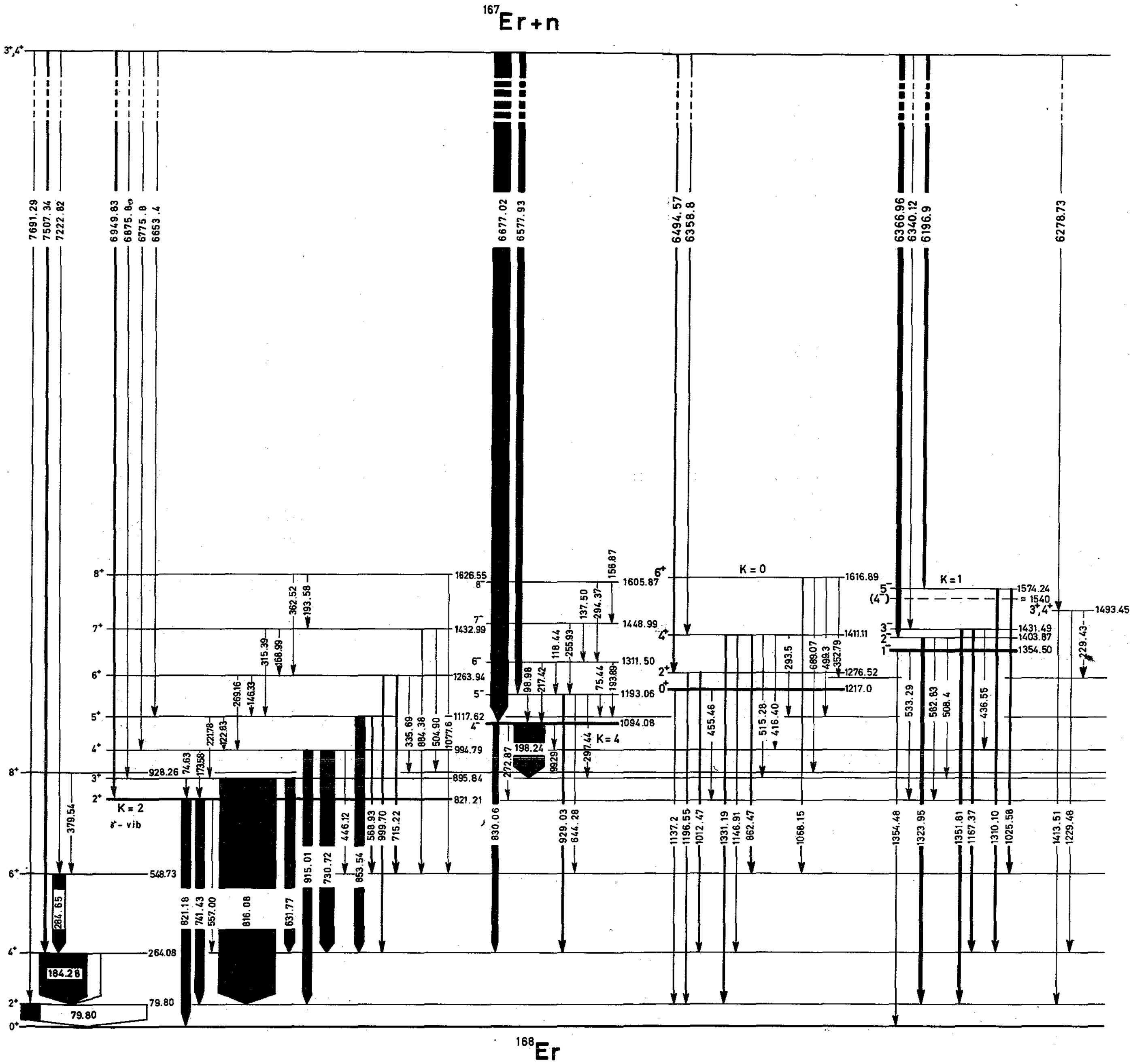
167Er+n
168Er
K = 2
γ - vib
K = 4
K = 0
K = 1
7691.29
7507.34
7222.82
6949.83
6875.8
6775.8
6653.4
6677.02
6577.93
6494.57
6358.8
6366.96
6340.12
6196.9
6278.73
79.80
264.08
548.73
821.21
895.84
928.26
994.79
1117.62
1263.94
1432.99
1626.55
1094.08
1193.06
1311.50
1448.99
1605.87
1217.0
1276.52
1411.11
1616.89
1354.50
1403.87
1431.49
1574.24
≈ 1540
1493.45
184.28
284.65
379.54
821.18
741.43
557.00
816.08
631.77
915.01
730.72
446.12
853.54
568.93
999.70
715.22
335.69
884.38
504.90
1077.6
74.63
173.58
221.78
122.83
269.16
146.33
315.39
168.99
362.52
193.58
830.06
272.87
198.24
98.98
217.42
99.29
118.44
255.93
297.44
137.50
294.37
75.44
193.89
156.87
929.03
644.28
1137.2
1196.55
1012.47
455.46
1331.19
1146.91
862.47
515.28
416.40
293.5
1068.15
689.07
499.3
352.79
1354.48
533.29
1323.95
582.83
508.4
1351.81
1167.37
436.55
1310.10
1025.58
1413.51
1229.48
229.43

Fig. 7a

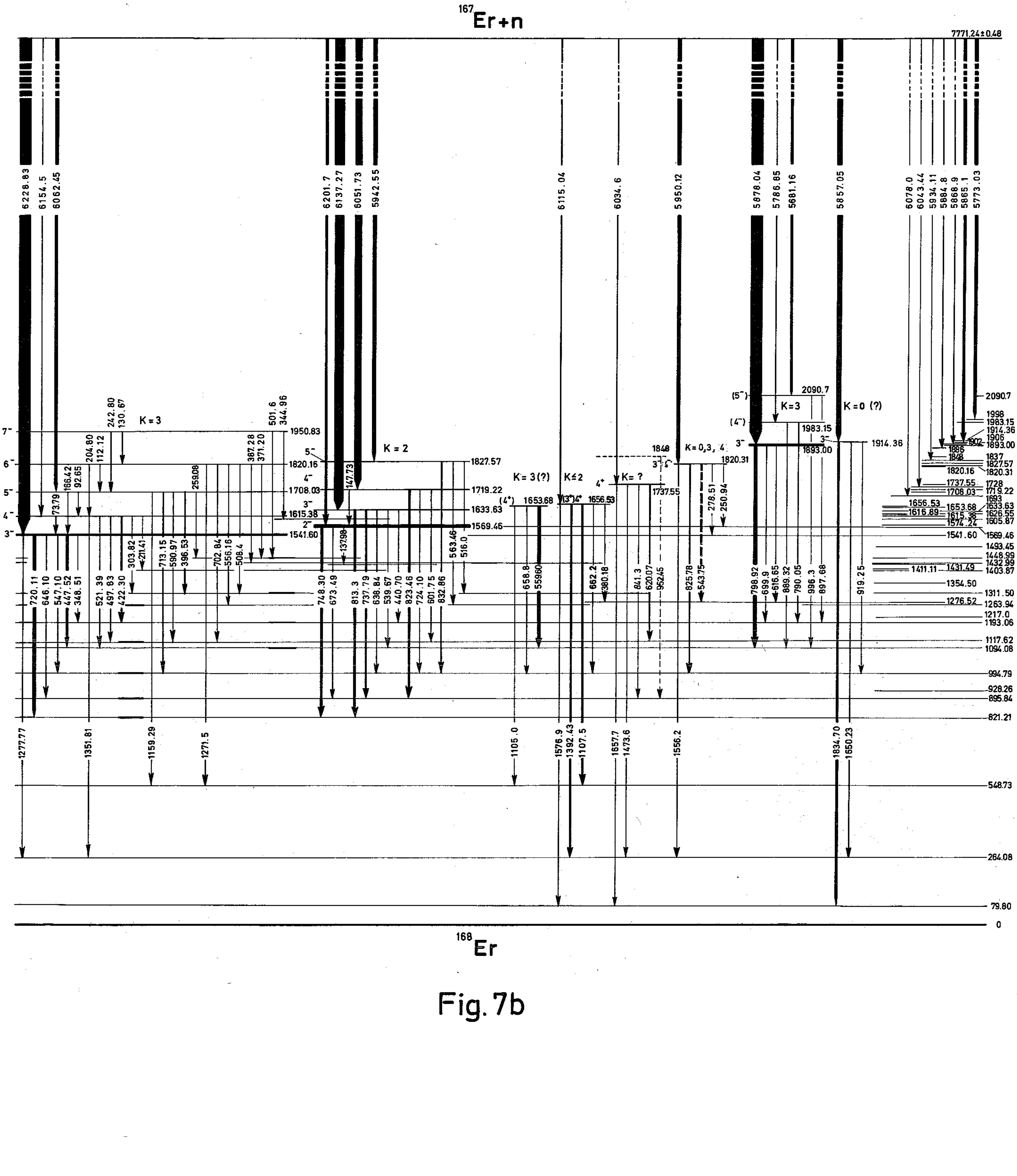

$^{167}Er+n$
7771.24±0.48
K = 3
K = 2
K = 3 (?)
K≤2
K = ?
K = 0,3, 4
K = 3
K = 0 (?)
1541.60
1615.38
1708.03
1820.16
1950.83
1569.46
1633.63
1719.22
1827.57
1653.68
1656.53
1737.55
1848
1820.31
1893.00
1983.15
2090.7
1914.36
821.21
895.84
928.26
994.79
1094.08
1117.62
1193.06
1217.0
1263.94
1276.52
1311.50
1354.50
1403.87
1411.11
1431.49
1432.99
1448.99
1493.45
548.73
264.08
79.80
0
^{168}Er

Fig. 7b

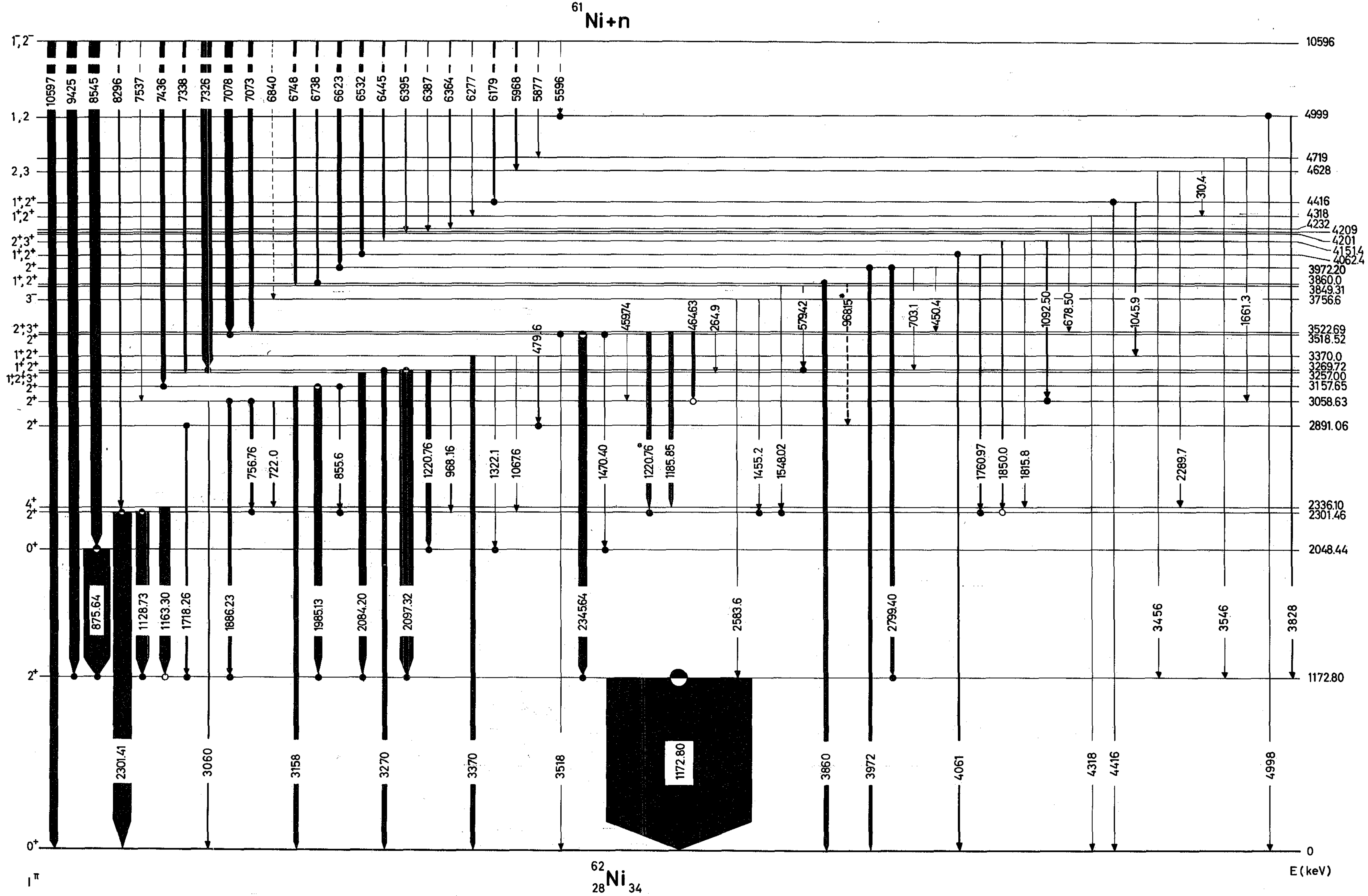
61Ni+n
62 28 Ni 34
I π
E (keV)
10596
4999
4719
4628
4416
4318
4232
4209
4201
4151.4
4062.4
3972.20
3860.0
3849.31
3756.6
3522.69
3518.52
3370.0
3269.72
3257.00
3157.65
3058.63
2891.06
2336.10
2301.46
2048.44
1172.80
0

Fig. 8

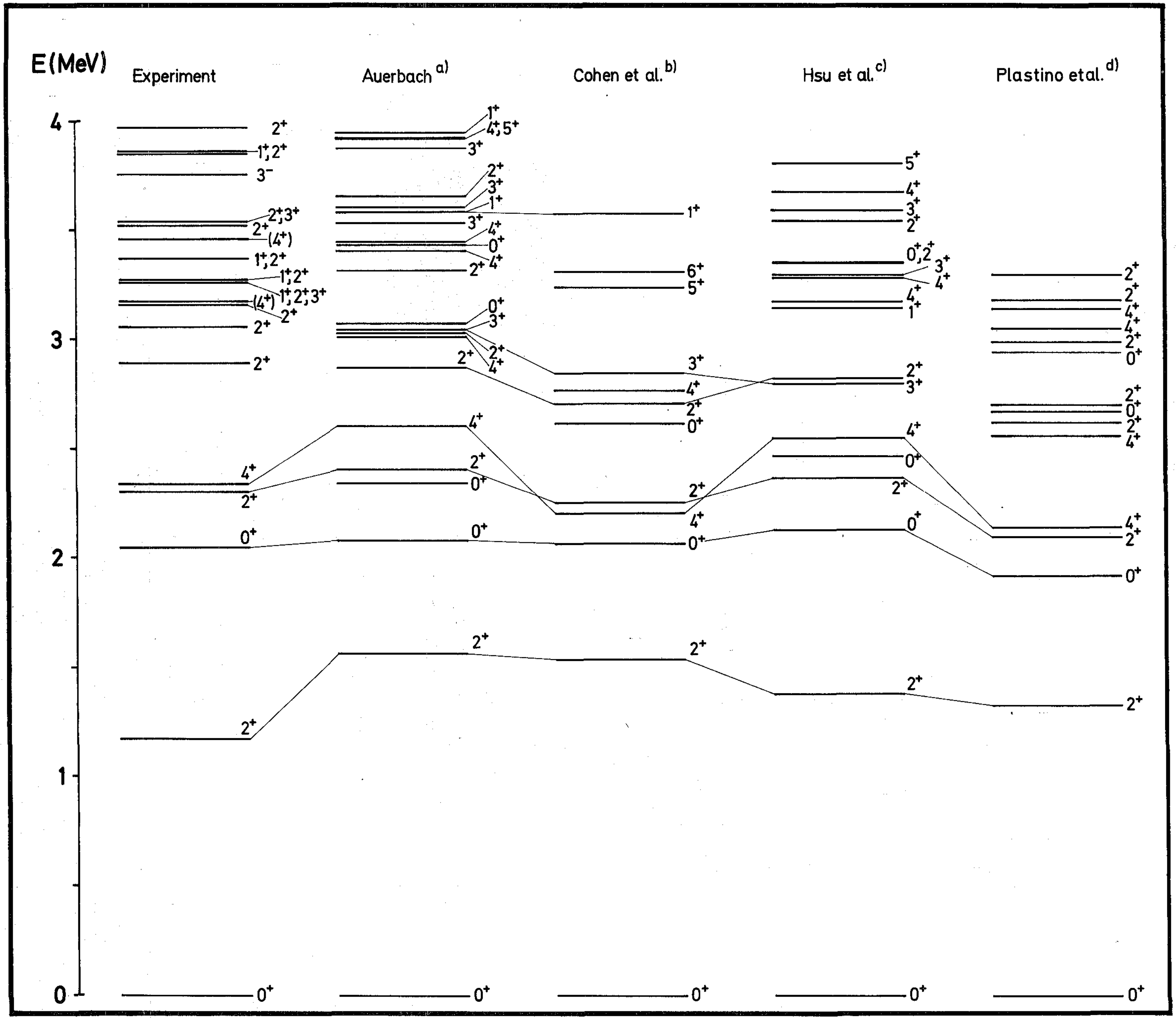

E(MeV)
Experiment
Auerbach a)
Cohen et al. b)
Hsu et al. c)
Plastino et al. d)

Fig.9

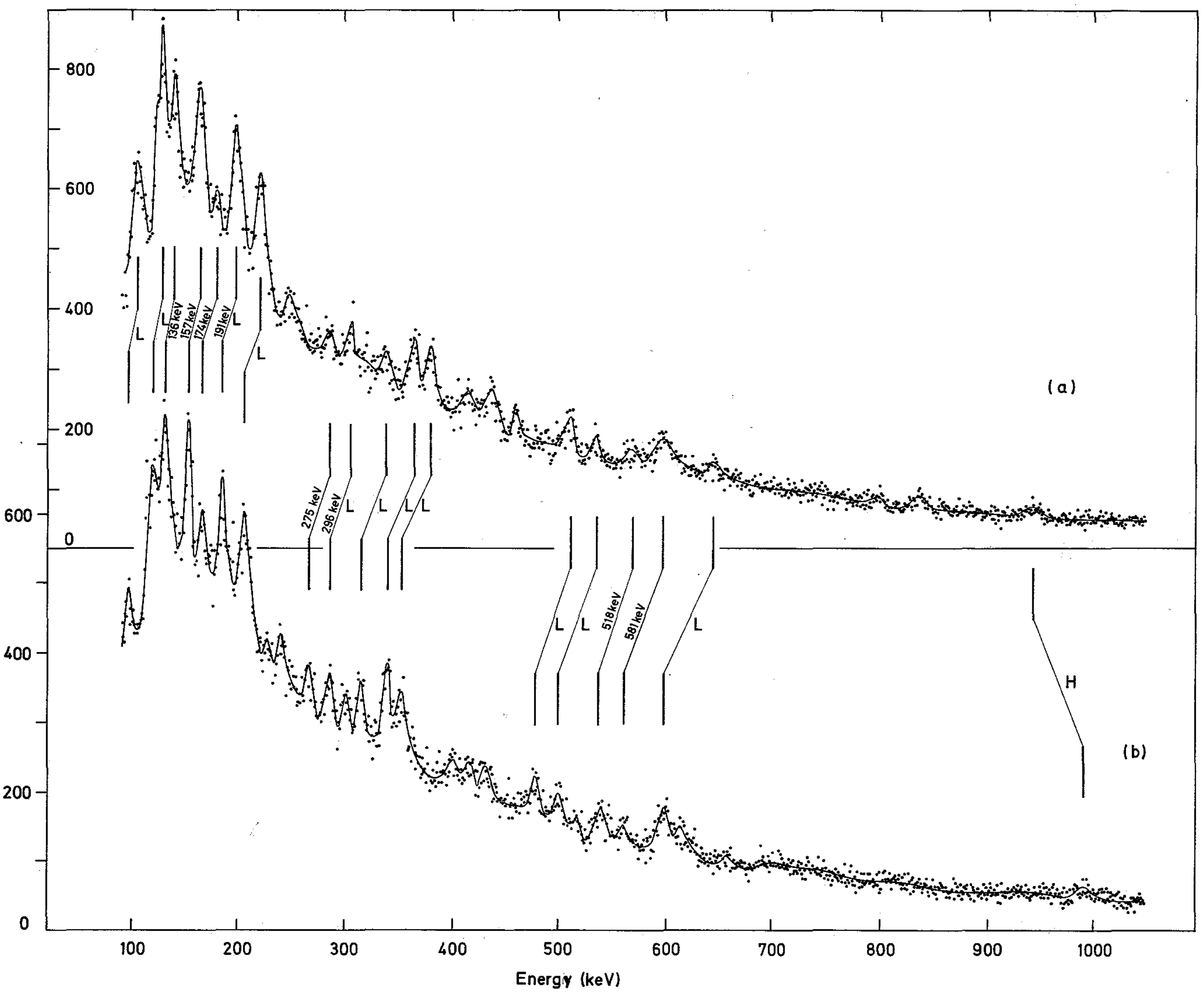

800
600
400
200
600
0
400
200
0
136 keV
157 keV
174 keV
191 keV
275 keV
296 keV
518 keV
581 keV
L
H
(a)
(b)
100
200
300
400
500
600
700
800
900
1000
Energy (keV)

Fig.10